FAST ION RELAXATION IN ITER MEDIATED BY ALFVÉN INSTABILITIES

N.N. GORELENKOV
Princeton Plasma Physics Laboratory, Princeton University, Princeton, NJ 08543, United States of America
Email: ngorelen@pppl.gov
V.N. DUARTE, M.V. GORELENKOVA
Princeton Plasma Physics Laboratory, Princeton University, Princeton, NJ 08543, United States of America
Zh. LIN
University of California, Irvine, CA 92697, United States of America
S.D. PINCHES
ITER organization, Route de Vinon-sur-Verdon, CS 90 046 13067 St. Paul Lez Durance, France

Abstract

We address the critical issue for future burning plasmas of whether high energy fusion products or auxiliary heating beam ions will be confined for sufficiently long time to compensate for thermal plasma energy losses. This issue can be mediated by one of the most deleterious collective phenomena - the instability of low, sub-cyclotron frequency Alfvén eigenmodes (AEs), such as toroidicity-induced AEs and reversed shear Alfvén eigenmodes considered in ITER steady-state scenario. Using a revisited quasi-linear (QL) theory applied to energetic particle (EP) relaxation in the presence of AEs, we find that the AE instabilities can affect both neutral beam ions and alphas although the resulting fast ion transport is expected to be modest if classical particle slowing down is assumed. On the other hand, the QL theory predicts that the AE amplitudes will be enhanced by the background microturbulence whilst this study remains outside of this work scope due to significant numerical efforts required to evaluate these effects. We report on EP relaxation dynamics utilizing several tools: the comprehensive linear stability study of the sub-cyclotron Alfvénic spectrum as computed by the ideal MHD simulations of NOVA for the AE eigenproblem, drift kinetic NOVA-C calculations for wave-particle interaction and AE growth/damping rates, and the predictive quasi-linear modeling coupled with the global transport code TRANSP to assess the EP relaxation on the equilibrium time scale.

I. INTRODUCTION

The problem of energetic particle (EP, also referred here as energetic or fast ions) confinement in tokamaks is essential for a successful self-sustained controlled thermonuclear reactor. For example collective effects due to Alfvén eigenmodes (AEs) in ITER are expected to play a significant role on the relaxation of $3.52MeV$ fusion products, alpha particles, and $1MeV$ injected deuterium beam ions.

It has been recently noted that regimes of enhanced AE induced fast ion transport can occur, where the background microturbulence mediates this EP relaxation [1]. This points out to a

novel route to explain the fast ion relaxation losses beyond the scenarios described in "Energetic ion transport by microturbulence is insignificant in tokamaks" [2]. It has been demonstrated numerically that the microturbulence-driven EP pitch angle scattering can significantly increase the amplitude of AEs above the levels likely to be damaging for the ITER first wall [3].

Different reduced models can be used to simulate the multi-mode EP relaxation in burning plasma conditions. For example the critical gradient model [4, 5], which does not have the velocity space resolution, can be used nevertheless for fast evaluation of EP relaxation. The main problem with this model is that it requires validations which are not available in future devices such as ITER nor it can be generalized for varying plasma regimes in present day devices. Another model is a more detailed, resonance broadened quasi-linear (or RBQ) model that evaluates the EP relaxation in both energy and canonical toroidal momentum space in the presence of Fokker-Planck collisions and can include the pitch angle effective scattering and zonal flows due to the microturbulence [6]. RBQ is general enough and ready for applications in planned future fusion devices. Both models rely on AE linear instability growth rate calculations, e.g., using NOVA/NOVA-C [7] whereas RBQ can implement the effective EP pitch angle scattering, if available, which in the case of classical Coulomb collisions comes from NOVA-C simulations but needs to be enhanced by the contribution due to the background microturbulence [8].

It's important to highlight that, currently, RBQ simulations only consider the wave-particle non-linearity arising from fast ion interaction with Alfvén eigenmodes (AEs) and the resulting alteration of the energetic particle (EP) distribution function in the constants of motion space.

In ITER superalfvénic ions include the auxiliary deuterium beam heating ions and fusion born alpha particles needed in the plasma to replenish the thermal ion losses. The alpha particle distribution function is far from that of a typical beam or ion cyclotron resonance heating ions which are normally have narrow width in pitch angles, $\chi = v_{||}/v$, where $v_{||}$ is the parallel to the magnetic field component of the ion velocity and v is its absolute value. For example tangentially injected beam ions in ITER are predicted to have $\delta\chi \lesssim 0.1$ [9]. Comprehensive linear and nonlinear studies of AE stability were performed recently for ITER baseline scenario [10] where several important kinetic damping mechanisms were accounted for and their effects on EP relaxation were discussed in details. Those sources for dampings should be considered standard for reliable predictions of EP confinement in fusion-grade reactor devices. One of the damping mechanisms pointed out in that reference is the trapped electron collisional damping which sets boundary conditions at the plasma edge but is often ignored in benchmarks [11].

We note that an essential feature of EPs in fusion reactors including fusion charged products is their bootstrap current which can provide additional current drive needed in a tokamak reactors especially in spherical tokamaks (STs) [12]. Fusion product bootstrap current has a nonzero finite value at the plasma center that is important for STs. The fast ion current drive is extremely sensitive to the details of energetic ion distribution function in the constant of motion (COM) space requiring accurate modeling of AE driven diffusive and convective transport [13]. Those issues are vital for making credible projections for fusion reactors.

II. TAE/RSAE LINEAR STABILITY IN ITER STEADY-STATE SCENARIO

We start with the comprehensive linear stability analysis performed with the help of the ideal MHD code NOVA [14] and its hybrid drift kinetic extension NOVA-C [7]. NOVA ideal MHD analysis uncovers the Alfvénic eigenmodes in the frequency range spanning from the geodesic acoustic mode frequency up to the Ellipticity-induced Alfvénic Eigenmode gap. In Fig.1 we present the ITER steady-state plasma profiles prepared by the ASTRA code [15] and made available for simulations through the IMAS framework [16]. It was summarized in the IAEA presentation [17]. In the selected ITER steady state scenario, the only planned auxiliary heating and current drive schemes are Neutral Beam Injection (NBI) and Electron Cyclotron Heating (ECH) [15].

ITER steady-state operation is characterized by deuterium neutral beam injection (NBI) power $P_{NBI} = 33\ MW$ and the electron cyclotron heating and current drive power $P_{EC} = 20\ MW$. Unlike the baseline case scenario considered earlier [10], the present AE stability analysis accounts for an ITER steady-state scenario that is characterized by a fusion α-particle pressure profile twice as large and beam ion beta profile ten times larger. Developing the plasma control of the steady state scenario of interest involves various techniques to optimize the NBI current drive in particular [15]. Unsurprisingly the NBI contribution to AE instabilities was ignored in the follow-up studies [18, 19]. We stress here that the NBI current drive could be quite important factor for ITER operation even though the effect of AEs are shown here to be benign for EP ion confinement.

Both fast ion specie fusion α's and beam ions are included in our simulations. Their distribution contour maps are shown in Figs. 2 and are taken near the injection (birth) energies in the plane of canonical angular momentum, P_φ, and the normalized to EP energy adiabatic moment, $\lambda = \mu B_0/\mathscr{E}$. Given the ratio of their super-Alfvénic velocities to the Alfvén speed, it is expected that the AE instability drive will be maximized against $v_{\alpha,b0}/v_A$ ratio. Furthermore, one can see jumps at the separatrix between the passing and trapped alphas on the right figure. Those jumps are physical and they are due to the jumps in the drift orbit precession times associated with the transitions from trapped to passing ion orbits and vise versa. If multiplied by the precession times of the fast ions their "distribution function times the precession time" quantity becomes smooth function near the transition points and does not have those jumps.

We note that Figs.4, (a) and (b), are plotted on the same plane as Fig. 19 "Confinement loss domains in $\mu/\mathscr{E}$, P_φ" of Ref.[20], where various particle orbits are labeled. For instance, it is evident that the fast ions injected by NBI are exclusively composed of co-passing particles.

NOVA has found around 600 Alfvén modes of interest out of which NOVA-C identified 42 unstable or marginally stable eigenmodes for the subsequent RBQ runs. The AE stability is addressed by the kinetic NOVA-C code which incorporates rich physics including the background dampings and advanced fast particle representation that allowed favorable benchmarks against the main available stability codes [11]. We show AE growth rates in Fig. 3.

From the linear AE stability results several important observations can be made. First, our linear AE stability analysis is consistent with earlier results [18, 19] especially the toroidal mode number range of the unstable AEs and their characteristic growth rates. The growth rates have the

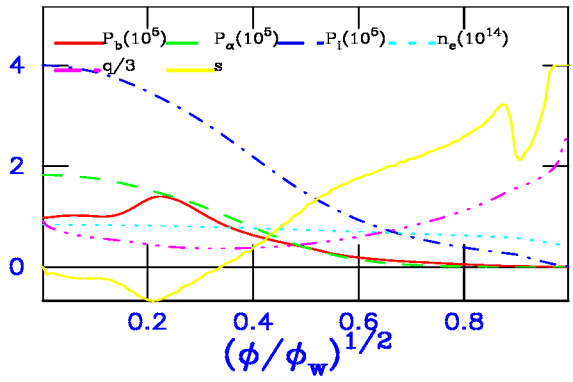

Figure 1. *Plasma profiles of ITER steady-state scenario used in simulations. Shown are the radial profiles of beam pressure, P_b, fusion product alpha particle pressure, P_α, thermal ion pressure P_i plotted in Pascals, electron density, n_e in units cm^{-3}, the safety multiplied by $1/3$, i.e. $q/3$, and the magnetic shear $s = q'r/q$. Horizontal axis corresponds to the square root of the toroidal flux normalized to its value at the last closed surface.*

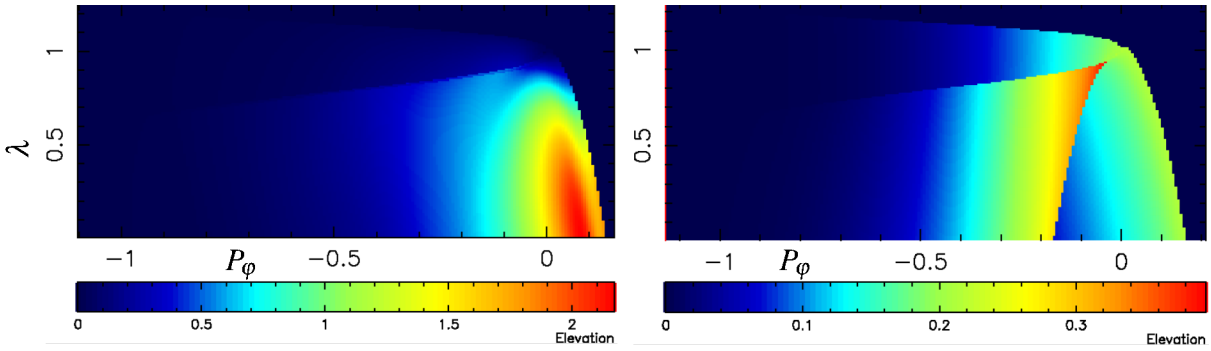

Figure 2. *Beam ion (left) and alpha particle (right) distribution functions shown as contour map in the plain of the toroidal canonical momentum P_φ and normalized to the ion energy adiabatic moment λ. Both distribution functions are the sums over different signs of EP parallel component of particle velocities, $v_\parallel/|v_\parallel|$. Notably, on the right panel the co-passing and counter-passing ions show discontinuity in DF values which is due to their precession time discontinuity.*

maximum or a rollover point at around $n = 20 \div 30$ in those calculations. Second, two regions in radius have strongest contributions to the growth rates: near the plasma center and near the q_{min} location. Third, the multiplicity of AEs and their resonances will likely result in the overlaps of the resonances in the constant-of-motion space due to the nonlinear amplitude broadening. Fourth, the dominant damping rate that controls the EP profiles near the edge, i.e. set the boundary conditions, is the trapped electron collisional damping. For reliable predictions such damping is required in simulations. Ignoring it would change the radial domain of EP confinement and, as a result, would overestimate the loss fraction of fast ions such as discussed in Ref.[21] where the critical gradient model (CGM) [5] was revisited. We would like to note that the mentioned CGM approach has

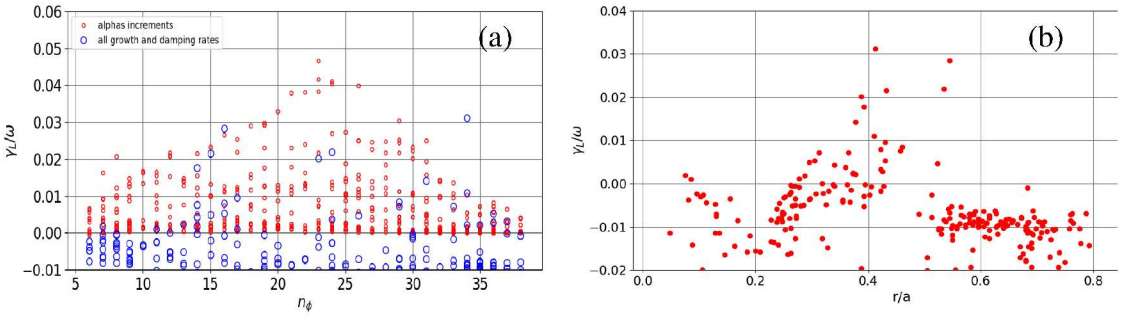

Figure 3. *Figure (a) shows the sum of AE growth and damping rates for each mode computed for the unstable and marginally stable Alfvén eigenmodes. They are shown as blue open circles. Net growth rates due to fusion α-particles only are shown as smaller red circles. AE net growth rates include beam ion drive. Figure (b) represents the AE growth rates as functions of the mode minor radius location of its maximum amplitude value.*

limitations. One of them is that it does not predict the AE amplitudes near the saturation. It also does not allow for the fast ion slowing down nor for EP pitch angle scattering in time. CGM can be considered as a limiting case of QL approach if the number of unstable AEs goes to infinity. This was shown in Ref.[4].

We include most of the linear dampings relevant to AE stability, including thermal ion and electron Landau damping, radiative damping, as well as the nonlinear (or QL) damping emerging when during the AE amplitude saturation. One of the dampings neglected in our calculations is the continuum damping. This approximation is not expected to change our conclusions concerning the fast ion relaxation since the most unstable AEs have high-n toroidal mode number whose continuum damping is negligible [22]. We discuss this approximation in details in Appendix A.

III. QUASI-LINEAR MODELING OF FAST PARTICLE RELAXATION

The recently built numerically efficient, self-consistent quasi-linear (QL) code RBQ is applied to ITER steady-state scenario [15]. It is capable of addressing the EP confinement in the presence of several to multiple Alfvénic modes by following the time evolution of their amplitudes and by advancing the EP distribution function in the space of the invariants of the unperturbed motion. This can be done either within the RBQ code itself or by providing the diffusion and convective coefficients for the subsequent calculation by Whole Device Modeling (WDM) package such as NUBEAM [23] which has rich physics. Furthermore, the RBQ code has been interfaced with the WDM TRANSP code and has preliminarily shown to agree well with experimental measurements when applied to DIII-D critical gradient experiments [6]. In the NUBEAM guiding-center orbit following simulations, RBQ transport coefficients are applied while maintaining the same wave-particle nonlinearity utilized in RBQ model.

RBQ solves the system of equations (published earlier for 2D, i.e. $\mathbb{R}^2$ case [6]) assuming the

ansatz for the harmonics of the perturbed quantities $e^{-i\omega t-in\varphi+im\theta}$. For a single mode in tokamaks, the QL diffusion of an ion occurs in $\mathbb{R}^1$ slanted direction near each resonance along the paths of constant values of the expression [24]:

$$\omega P_\varphi + n\mathscr{E} = \text{const}, \tag{1}$$

where ω and n are the angular frequency and the toroidal mode number of a mode respectively. One immediate consequence of this expression is that at positive values of n increasing P_φ, i.e. the EP diffusion to the plasma edge, leads to decreasing EP energy. In other words, this is how the unstable system transfers the energy to the eigenmode.

Following Ref.[25] we denote each analyzed mode with the symbol k and corresponding resonances with the symbol $\boldsymbol{l}$. The latter denotes the resonance diffusion region by the index of the poloidal harmonic and by the index of the poloidal sidebands, hence being a vector.

If the ensemble of modes is known, the distribution function evolves according to the following QL equations implemented in RBQ. The system of QL equations in its general form is given in Ref.[26]. It was adopted to NOVA-C notations in Refs.[25, 27] which was generalized for 2D case as:

$$\frac{\partial f}{\partial t} = \hat{L}(f, f_0) = \sum_{k,\boldsymbol{l}} \frac{\partial}{\partial I_k} D_{\boldsymbol{l}}(I_k;t) \frac{\partial}{\partial I_k} f + \sum_k \nu_\perp R^2 \left\langle v^2 - v_\parallel^2 \right\rangle \frac{\partial^2 (f - f_0)}{\partial I_k^2}, \tag{2}$$

where the diffusion coefficients are:

$$D_{\boldsymbol{l}}(I_k;t) = \pi C_k^2(t)\, \mathscr{E}^2 \frac{\mathscr{F}_{\boldsymbol{l}}(I_k - I_{kr})}{\left|\frac{\partial \Omega_l}{\partial I_k}\right|_{I_{kr}}} G^*_{km'p} G_{kmp}, \tag{3}$$

and where $\nu_\perp$ is the 90^0 pitch angle scattering rate frequency, f and f_0 are the distribution functions at times t and $t = 0$ respectively, $\mathscr{F}_{\boldsymbol{l}}$ is the resonance window function, G_{kmp} are the wave particle interaction (WPI) matrices, and Ω_l is the resonance frequency of WPI between the mode k and the resonant ion. In earlier 1D version RBQ used the action variable $I_k = \mathscr{E}/\omega_k - P_\varphi/n_k \simeq -P_\varphi/n_k$, i.e. as a toroidal canonical momentum divided by $-n_k$ ignoring energy dependence [6, 25]. Also here I_{kr} is the action at a given resonance. Subindex k denotes that the action is related to k-th mode. In general three action variables can be used within the RBQ framework, i.e. $\hat{L}$ operates in 2D plane, $\hat{L} : \left\{ \left(P_\varphi, \mathscr{E}\right) \in \mathbb{R}^2 \right\}$ at each value of μ. In the current version of RBQ2D we consider the sub-cyclotron frequency range implying that $\mu = \text{const}$ for the operator $\hat{L}$. Also unlike the recent revision of the QL theory [28], Eq.(2) includes only the diffusion terms ignoring the convective velocities which require the knowledge of zonal flows (ZF). ZF modifications of RBQ model are straightforward if the convective velocities are known but are beyond the scope of this paper.

The equation for the amplitude of each mode can be written formally without the explicit contributions from other modes though such contributions are mediated by the fast ion distribution function. The amplitudes of the modes of interest evolve according to the set of equations:

$$\frac{dC_k^2(t)}{dt} = 2\left(\gamma_{L,k}(t) + \gamma_{d,k}\right) C_k^2(t), \tag{4}$$

where $\gamma_{L,k}$ and $\gamma_{d,k}$ are linear growth and damping rates of the k-th mode at time t, and $C_k = \delta B_{\theta,k}/B$ is the amplitude of that mode. The AE damping rate is considered as constant in time but it can change in principle on a slow time scale during the RBQ evolution.

The RBQ model is designed for applications using both isolated and overlapping modes whereas the conventional quasilinear theory applies to the multiple overlapping modes. We use the same structure of quasilinear equations for the ion distribution function evolution [26, 29, 30] but with the resonance delta function broadened over some region in the direction of the action I_k variation:

$$\delta\left(I_k - I_{kr}\right) \to \mathscr{F}_{\boldsymbol{l}}\left(I_k - I_{kr}\right). \tag{5}$$

Resonance broadening function $\mathscr{F}_{\boldsymbol{l}}$ is the key novel element of the proposed diffusion model whose parametric dependencies are verifiable against known analytic asymptotic behaviors for isolated modes, see Appendices of Ref. [6]. It satisfies the property $\int_{-\infty}^{+\infty} \mathscr{F}_{\boldsymbol{l}}\left(I_k - I_{kr}\right) / \left|\frac{\partial \Omega_l}{\partial I_k}\right|_{I_{kr}} d\Omega_l = 1$ pointed out in [31].

If the diffusion occurs approximately along P_φ, i.e. in the low mode frequency approximations, the whole problem reduces to the set of one-dimensional equations, that is discussed in the Fitzpatrick's thesis [29] (in addition see Ref.[32] where the window function was introduce in its preliminary form revisited in Ref.[31]). The effect of several low-n modes on energetic particles cannot be accurately determined without numerical simulations that capture the diffusion in two dimensional space, $\left\{\left(P_\varphi, \mathscr{E}\right) \in \mathbb{R}^2\right\}$. This is due to the complex multi-directional diffusion dynamics of the resonant ions in $\mathbb{R}^2$ space and possible resonance overlap in the presence of multiple AEs. Thus this 2D generalization is a major extension target for the RBQ model.

We applied the RBQ to ITER steady-state plasma characterized by 42 unstable or marginally stable AEs and prepared the COM diffusion coefficients for WDM processing. Both beam ion and alpha particle plasma components contribute to the AE drive although the linear stability analysis indicates that beam ions have on average the growth rate twice as high. This is because beam ions are injected into the most unstable location in the COM space and almost all the beam ions are passing and easily resonate with AEs.

RBQ pre-computed diffusion coefficients turned out to be quite large and localized where most of 42 tested AE modes are unstable or marginally unstable, i.e. near the q_{min} point, reaching values up to $50 m^2/sec$ in the COM space and going down to $\sim 1 m^2/sec$ at the periphery. This implies the local flattening of EP profiles near q_{min} but overall the EP redistribution, and losses in particular, can be modest.

Fig.4 shows time evolution during EP relaxation corresponding to AEs driven purely by the injected beam ions, i.e., this is the case of pure beam ion drive unassisted by fusion alphas. We have found that the amplitudes of AE modes are quite small reaching values $\delta B_\theta/B \sim 10^{-5} \div 10^{-3}$. As a result, no significant beam ion losses to the wall were present in NUBEAM simulations. At the same time the analogous, unassisted AE drive by fusion alphas showed very weak amplitude modes at $\delta B_\theta/B < 10^{-4}$.

In contrast to the unassisted AE drives let's consider more relevant to experimental expectations

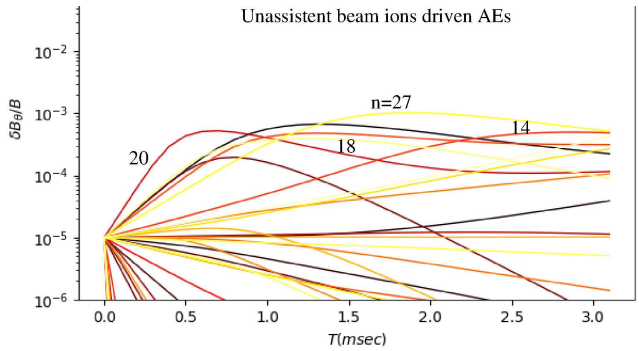

Figure 4. *Initial, overshooting time period of AE evolution of unstable and marginally unstable modes prepared by the NOVA/NOVA-C suite of codes and processed by the RBQ2D quasi-linear code over* 3 *msec time window. Toroidal mode numbers of some of the most unstable modes are indicated on the figure.*

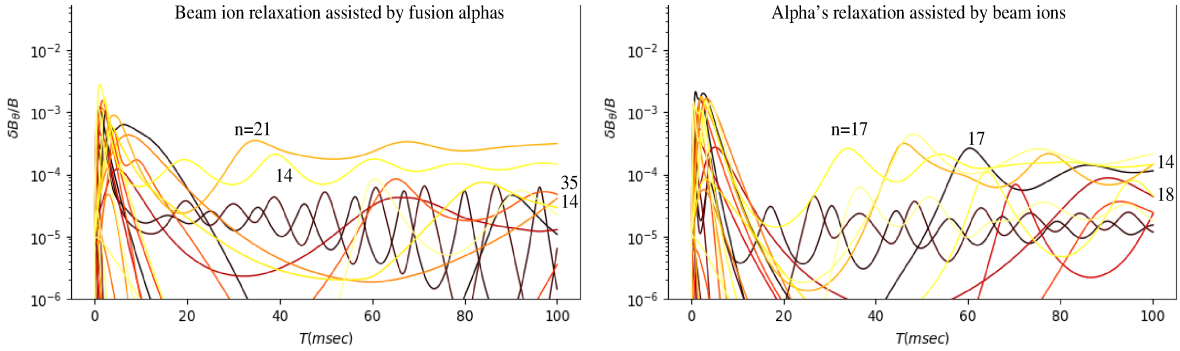

Figure 5. *The same as in Fig.4 but characterized by longer RBQ simulation times in order to see the AE saturation. The* Alfvén *modes are driven by both beam ions and fusion alphas. Figure (a) corresponds to the case when beam ions are relaxed whereas the AE growth rates include alpha particle drive. Figure (b) corresponds to alpha's DF relaxation assisted by beam ion drive.*

the case of AE instabilities when both fusion alphas and beam ions contribute to the drive. In this case the AE amplitude time evolution is shown in Figs.5. We follow the QL theory prescription[26] which controls DF evolution according to the equations written for that specie. It follows from these figures that the slowing down beam ions together with fusion alphas particles drive AEs to higher amplitudes in comparison to the overshoot case, up to $\delta B_\theta/B \lesssim 3\times 10^{-3}$. With AE amplitudes prepared by the RBQ code the diffusion coefficients were transferred to the NUBEAM Monte-Carlo package whose calculations are discussed in Sec.V. It is important to note that the initial saturation level we see in RBQ simulations at $t = 1.5 \div 3$ *msec* (see Fig.4) corresponds to the case when the EP profiles are still far from the relaxed state and thus the AE amplitudes are still converging to the saturated state. Also, it is interesting that both cases represented in Figs.5 (a) and (b) have approximately the same values of AE amplitude at saturation that is they are determined primarily by the values of AE growth rates which are the same in both cases.

IV. NUBEAM GYRO-CENTER SIMULATIONS OF FAST BEAM ION AND FUSION ALPHA PARTICLE SLOWING DOWN

Ideally the EP relaxation for WDM simulations should include EP distribution function in COM space evolving in time on a scale that includes three characteristic times: inverse linear AE growth rate, damping rate and effective pitch angle scattering rate [33]. Such dynamics was demonstrated and is well captured by the QL theory implemented in RBQ simulations [1]. Having this approach in mind in the longer term we aim at the steady state plasma operation regimes but ignore such intermittent behavior.

This approach can unify different simulations of several initial value codes such as used in recent comprehensive benchmark [11] by making use of the WDM prototype NUBEAM package [23]. It requires the following diffusion and convective transport coefficients to be recorded in simulations [34] by either the reduced models such as RBQ or by initial value codes discussed in Ref.[11]:

$$D_{\bar{P}_\varphi \bar{P}_\varphi}, D_{\bar{P}_\varphi \bar{\mathscr{E}}}, D_{\bar{\mathscr{E}}\bar{\mathscr{E}}} \tag{6}$$

$$C_{\bar{P}_\varphi}, C_{\bar{\mathscr{E}}}, \tag{7}$$

where $D_{\bar{x}\bar{y}}$ being the diffusion and $C_{\bar{x}}$ being the convective motion coefficients of fast ions due to the AE activity, collisions or due to the associated zonal flow (ZF). Here the over-bar symbol $^-$ means that the value is normalized to either $\psi_{\theta w}$ for canonical momentum or to either the EP birth or the injection energy $\mathscr{E}_0$ for the EP kinetic energy.

We note that coefficients D, C need a special rule for implementation in NUBEAM to describe the resonance ion motion in the COM space, since COM coordinates are specific for each specie under consideration. They are given by well a known expression if one AE is the only mediator which follow from Eq.(1):

$$n\Delta\bar{\mathscr{E}} = -\omega\Delta\bar{P}_\varphi, \tag{8}$$

keeping $\mu = const$. The minus sign here implies that the resonant particle is losing its energy when $\bar{P}_\varphi$ increases, i.e. the resonant ion moves towards the edge and loses its energy to drive the instability. The WPI is the only case relevant to fusion plasmas when other scattering mechanisms are negligible such as when the turbulence-induced scattering is small and the AE/EP system goes into the frequency chirping regime [35]. For Alfvénic oscillations the eigenmode frequency is typically small, much smaller than the cyclotron frequency of plasma ions, so that it is quite safe to assume $\left|\Delta\bar{\mathscr{E}}/\bar{\mathscr{E}}\right| \ll \left|\Delta\bar{P}_\varphi/\bar{P}_\varphi\right|$ for analytic estimates, if needed.

The above condition, Eq.(8), needs to be enforced for EP relaxation. One way to do this is relevant to the cases when the required bins to describe EP distribution function in the COM space are large, such as extensively used in the kick model [36]. In that case a special probability density function has to be introduced to differentiate resonance ions from the non-resonant ones. That scheme adds the dimensionality and complexity to the problem.

Another route when the dimensions of the problem can be sufficient to resolve EP dynamics. Let us consider the required for NUBEAM simulations COM grid bins which contain N points

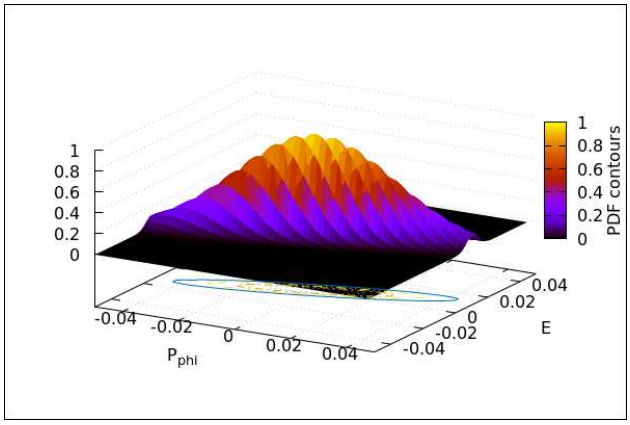

Figure 6. *PDF example for* $\rho = 0.9$, $\sigma_{\bar{P}_\varphi} = 0.015$, $\sigma_{\bar{\mathscr{E}}} = 0.005$.

with $\bar{P}_\varphi$ and $\bar{\mathscr{E}}$ grids being equidistant such as in NOVA-C/RBQ model. That dimensions fixed in our problem are $N_{P_\varphi} = 200$ and $N_{\mathscr{E}} = 40$. Then we construct the local bin probability density function (PDF) characterized by the COM location as:

$$p = \frac{\sqrt{1-\rho^2}}{\pi \sigma_{\bar{P}_\varphi} \sigma_{\bar{\mathscr{E}}}} \exp\left\{ -\left[\left(\bar{P}_\varphi - \bar{P}_{\varphi 0}\right)^2 / \sigma^2_{\bar{P}_\varphi} + \left(\bar{\mathscr{E}} - \bar{\mathscr{E}}_0\right)^2 / \sigma^2_{\bar{\mathscr{E}}} - 2\rho \left(\bar{P}_\varphi - \bar{P}_{\varphi 0}\right)\left(\bar{\mathscr{E}} - \bar{\mathscr{E}}_0\right) / \sigma_{\bar{P}_\varphi} \sigma_{\bar{\mathscr{E}}} \right] \right\}, \tag{9}$$

where $0 < \rho < 1$, so that at $\rho = 0$ the resonant ion can experiences a "kick" from i, j cell with equal probability of moving in $\left(\bar{P}_\varphi - \bar{P}_{\varphi 0}\right)/\sigma_{\bar{P}_\varphi}$ or $\left(\bar{\mathscr{E}} - \bar{\mathscr{E}}_0\right)/\sigma_{\bar{\mathscr{E}}}$ directions over Δt time step. The PDF function needs to be normalized:

$$\int d\bar{P}_\varphi d\bar{\mathscr{E}}\, p = 1. \tag{10}$$

An example of such PDF is given graphically in Fig.6. If $\rho = 0.9$, the natural for the WPI slanted direction is enforced as shown in Eq.(8) which is close to (and it is exact at $\rho = 1$)

$$n\sigma_{\bar{\mathscr{E}}} = -\omega \sigma_{\bar{P}_\varphi}.$$

In the near threshold case, i.e., when the diffusion is primarily in the $\bar{P}_\varphi$ direction, it needs to be corrected by an additional $\bar{\mathscr{E}}$ diffusion by the amount given in Eq.(8).

Thus, given the time step Δt the resonant ion is expected to have the diffusive change in the P_φ direction given by

$$\sigma_{\bar{P}_\varphi} = \sigma_1 \sqrt{D_{\bar{P}_\varphi \bar{P}_\varphi} \Delta t} \tag{11}$$

and a change in $\bar{\mathscr{E}}$:

$$\sigma_{\bar{\mathscr{E}}} = \sigma_2 \sqrt{D_{\bar{\mathscr{E}}\bar{\mathscr{E}}} \Delta t} \tag{12}$$

where the signs $\sigma_1 = \pm 1$ and $\sigma_2 = \pm 1$ are independent from each other and determined randomly. Another change it will experience is due to the convective motion in P_φ direction given by $C_{\bar{P}_\varphi} \Delta t$

and in $\bar{\mathscr{E}}$ direction: $C_{\bar{\mathscr{E}}}\Delta t$. The random steps in COM variables of NUBEAM are natural for the Monte-Carlo technique.

In this paper we follow the third way to implement the transport coefficients D, C in NUBEAM calculations which we describe below. Since the EP diffusion (and convection) is found for each cell and fast ions diffuse (and convectively move) according to the pre-computed values of D, C, each ion at a grid point (grid cell or *narrow* bin) $\bar{P}_\varphi, \bar{\mathscr{E}}$ diffuses with the coefficient D and at the same time experiences convection C.

Then we prescribe for the particle kicks the following changes in COM variables

$$\Delta\bar{P}_\varphi = \sigma_1\sqrt{\Delta t D_{\bar{P}_\varphi\bar{P}_\varphi}} + C_{\bar{P}_\varphi}\Delta t \equiv \Delta\bar{P}_{\varphi D} + C_{\bar{P}_\varphi}\Delta t,$$

$$\Delta\bar{\mathscr{E}} = -\sigma_1\sqrt{\Delta t D_{\bar{\mathscr{E}}\bar{\mathscr{E}}}} + \sigma_2\left(\frac{-D_{\bar{P}_\varphi\bar{\mathscr{E}}}}{\sqrt{D_{\bar{\mathscr{E}}\bar{\mathscr{E}}}D_{\bar{P}_\varphi\bar{P}_\varphi}}} - 1\right)\sqrt{\Delta t D_{\bar{\mathscr{E}}\bar{\mathscr{E}}}} + C_{\bar{\mathscr{E}}}\Delta t,$$

or

$$\Delta\bar{\mathscr{E}} = -\left(\sigma_1+\sigma_2\right)\sqrt{\Delta t D_{\bar{\mathscr{E}}\bar{\mathscr{E}}}} - \sigma_2\sigma_1\frac{D_{\bar{P}_\varphi\bar{\mathscr{E}}}\Delta t}{\Delta\bar{P}_{\varphi D}} + C_{\bar{\mathscr{E}}}\Delta t.$$

This complicated recipe warrants the slanted path in COM EP diffusion, Eq.(8). It may not be always possible to distinguish the EP diffusion from convection in the initial value codes such as GTC or GYRO. In those cases prescribing EP motion through the convection seems reasonable but more often exchange of EP convection will be required.

The representation of the EP motion during the transport processes in terms of its diffusive and convective kicks could be considered as a simplification if the characteristic time scale and the spacial grids are large. But with sufficient grid resolution the above representation, Eqs.(6,7), seems to be adequate for the problems of interest. Another simplification for this problem is that coefficients D, C are the sums of the contributions from several resonances since AEs have global mode structures.

The optimization of this model with regard to the time step Δt can also be done for example the following way. The main limitation of Monte-Carlo simulation is coming from the requirements that the diffusion/convection steps should not be larger than the grid size $\Delta\bar{\mathscr{E}} < N_{\mathscr{E}}$, $\Delta\bar{P}_\varphi < N_{P_\varphi}$. Moreover, since for the Alfvénic oscillations and associated WPI the ion motion is primarily expected in P_φ direction one would expect that the choice of the time step can be made according to the requirement on the radial kick. We, thus, can write it as

$$\Delta t = N^2_{P_\varphi} D^{-1}_{\bar{P}_\varphi\bar{P}_\varphi}. \tag{13}$$

V. BEAM IONS AND FUSION ALPHAS ARE DEPLETED AT THE PLASMA CORE BY AES

We apply the NUBEAM, Monte-Carlo guiding center-orbit-following package, to compute the confined alpha particle and beam ion density profiles which are typically monotonic in radius as shown in Fig.7 by the solid curves. When the AE diffusion prepared by the RBQ is turned on

NUBEAM finds that EP profiles of both alpha particles and beam ions become depleted near the plasma center as shown by the dashed lines on the graph. Perhaps this is the most important implication of the effect of the Alfvénic modes on fast ion confinement in the tokamak plasmas in ITER found so far. According to our calculations, the AE driven losses are expected to be negligible for beam ions whereas for alphas they are found to be around 1.7%. This is likely due to the significant fraction of trapped alphas in comparison with beam ions which are primarily passing, see Figs.2. Trapped alphas deviate by $2q\rho_{Lh}/\sqrt{r/R}$ from the magnetic surface whereas passing ions stay closer deviating by $q\rho_{Lh}$ in radial direction [24] where we denoted ρ_{Lh} the fast ion Larmor radius.

Another important factor missed in our calculations in comparison with our own results applied to DIII-D [6] is the absence of robust evaluations of the additional, effective pitch angle scattering which needs to be included using dedicated efforts for ITER. This seems to be a concern for future applications of many reduced simulations which need to rely eventually on the values of thermal electron and ion conductivities. In our study they are based on TRANSP calculations which may be far from expected in ITER experiments. This concern is a further motivation to study experimentally and theoretically the effect of the microturbulence on MeV ions in ITER.

Nevertheless we will use what exists in the literature, and in particular in Ref.[37] where the required effective scattering frequency of fast ions is based on simulation by the GS2, GYRO and GKW codes. If we follow this route we make use of the thermal ion and electron conductivities found by the TRANSP, which are $\chi_i = 4.2 * 10^3 cm^2/sec$ and $\chi_e = 4.9 * 10^3 cm^2/sec$. Also TRANSP has found that the thermal electron temperature $T_e = 27.6keV$ at the q_{min} location which is $r/a = 0.345$ in the run of interest. We find that the effective pitch angle scattering rate is $0.026 msec^{-1}$ for beam ions and $0.013 msec^{-1}$ for alpha particles. Given this uncertainty, we fix it uniformly in radius to $0.03 msec^{-1}$ for both species for long time RBQ simulations corresponding to $\Delta t = 100 msec$ which seems to be sufficient to address the steady state diffusion due to AE/EP interactions. Calculations using RBQ are still expensive and require runs on a PPPL computer cluster for several days whereas the NUBEAM with the RBQ diffusion rates requires an order of magnitude less time since no updates of the AE growth rates are required.

We have found that the fast ion slowing down relaxation using only classical, Coulomb scattering lead to insignificant density flattening near the q_{min} location. However, the most important effects is in the EP density depletion near the plasma center. This is true for both beam ion and alpha particle species having comparable injection or birth energies per nuclei which is about twice as larger as the energy corresponding to the Alfvén speed.

As previously mentioned RBQ simulations find that the saturated AEs with modest amplitudes, $\delta B_\theta/B \sim 10^{-5} \div 10^{-3}$, account for strong local radial diffusion which goes up to $\sim 50\ m^2/sec$ for resonant fast ions near q_{min}. However, near the plasma center the EP density is depleted, is likely due to finite orbit width effect to be comparable to the minor radius value in the central region. A similar depletion was reported in DIII-D beam ion profiles measured and simulated by the kick model [38]. Preliminary interpretation of this feature comes from the finite orbit width effects which are much larger in DIII-D than in ITER. This effect coupled with strongly driven

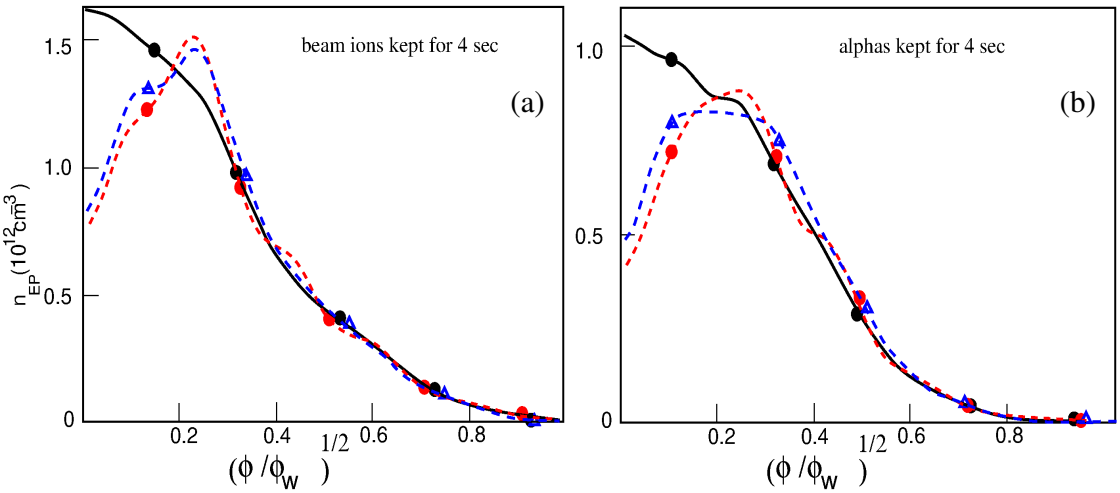

Figure 7. *Beam ion (figure a) and fusion alphas (figure b) density profiles prior (solid curves) and after AE saturation. The profiles are computed by the NUBEAM package with constant diffusion due to AEs over* 4 *seconds. When the EP diffusion coefficients are taken as corresponding to the overshoot region, i.e. around* 2 *msec time (see Figs.4,5) EP profiles are shown as red dashed curves. Whereas the EP profiles corresponding to the long time saturated phase, i.e. around* 100 *msec on Fig.5, NUBEAM predict profiles shown as blue dashed curves.*

AE diffusion of several radially overlapping modes near the center and relatively weak Coulomb pitch angle scattering result in EP profile inversion obtained by the NUBEAM package.

We see somewhat similar effect in ITER simulations. To illustrate this conjecture we write the WPI resonance condition for fast *MeV* energy ions we simulate with the NOVA-C code [7]. The WPI resonance condition reads:

$$\omega - k_{\|}v_{\|} - k_{\perp}v_{dr} + lv_{\|}/qR = 0, \tag{14}$$

where v_{dr} is the EP drift velocity and l is an integer. In conventional tokamak experiments on present day devices the dominant resonance contributions is due to two resonances, $|v_{\|}| = v_A/3$ and $|v_{\|}| = v_A$ corresponding to $l = \pm 1$ [7, 39, 40]. That case corresponds to $|k_{\|}v_{\|}| \gg |k_{\perp}v_{dr}|$ which is typical for DIII-D [38].

When that inequality is reversed the contributions of the side-bands to AE growth rate becomes dominant. This is also the case for the modes we find in ITER simulations, see Figs.5, $n = 15 \div 20$ in the saturated state. That is $v_{\alpha,b0}l/qR \simeq qn\rho_{Lh}v_{\alpha,b0}/rR$ near the plasma center. It implies that $r/a \simeq q^2/l$ which is true for higher order side-bands expected at the plasma center $l > 1$.

The consequences of the central region density depletion are not severe for the plasma power balance since no significant losses are found. What may be more important for the plasma discharge from the point of view of AE excitation is their effect on the current drive. Indeed the co-injection of beam ions plays an important role in creating and maintaining the reversed safety factor profile. As a result, the beam ion depletion in the plasma center can pose severe limitations to the steady-state scenario.

VI. SUMMARY

We performed a comprehensive stability analysis of ITER steady state plasma using the ideal MHD code NOVA, its drift kinetic extension NOVA-C and the recently developed two-dimensional QL code RBQ which employs a novel and revised methodology. This analysis helps to evaluate the AE saturation amplitudes and the relaxation dynamics of energetic particles present in planned ITER operations when both EPs, i.e. super-thermal beam ions and fusion α-particles are included.

Calculations using NOVA and NOVA-C revealed 42 unstable and marginally stable AEs for the subsequent RBQ processing. The identified modes included RSAEs, TAEs and EAEs residing in the corresponding gaps of the Alfvén continuum. Results of linear stability analysis have shown that the most unstable AEs toroidal numbers span from $n = 1$ to $n = 40$ with relatively modest growth rates, $\gamma_L/\omega < 5\%$, which justify the application of the perturbative analysis. Those results also justify the subsequent QL analysis since most AE growth rates are not strong enough and the effect of zonal flow is not expected to change the EP relaxation [41].

The applications of RBQ in its 2D version have shown that the AE amplitudes remain relatively low, $\delta B_\theta/B < 3 \times 10^{-3}$, for all 42 analyzed modes. In its current version, RBQ provides the AE diffusion and convective coefficients for the subsequent analysis. In the final stage of our analysis, the NUBEAM package was applied to evolve the fast ion distribution functions more accurately in the COM space which means that NUBEAM evolved EPs on a slowing down time scale. This requires NUBEAM to account for EP slowing down in realistic ITER conditions, that is to follow EP slowing down for several seconds. Both RBQ distribution evolution and NUBEAM calculations have found that the EP confinement with the Coulomb scattering does not result in significant fast ion losses, which is consistent with earlier studies of the baseline calculations [18, 19]. However, we have found earlier that the background microturbulence can significantly boost the AE saturation amplitudes by broadening the phase-space locations near the WPI resonances [1, 6]. For example, AE amplitudes can go up significantly with the ~~icrease~~increase of the anomalous scattering, $\delta B_\theta/B \sim \nu_{eff}^2$ and as a results EP losses can increase. Such dependence of the fast ion relaxation on the microturbulence intensity, however, does not allow us to conclusively predict the fast ion confinement in ITER advanced steady state scenarios without having quantitative predictions for the background microturbulence levels.

We have identified a potentially important effect of AEs on EP confinement which is due to EP depletion near the plasma center. This effect is connected with the beam ion and fusion alpha particle current drives which will be also depleted near the center so that the generation of current drive is required for WDM simulations. A self-consistent analysis of plasma discharge including this effect is needed to evaluate its consequences for the plasma scenario.

In a summary, we have found that the beam ions injected at $1MeV$ lead to stronger AE growth rates in comparison with the effect of fusion alpha particles, which are born as the source that is isotropic in pitch angle. This was not the case in earlier studies of ITER baseline scenario [10] where NBI injected fast ions have much smaller (around ten times smaller) beta. On the other

hand, the background microturbulence can enhance EP losses in ITER plasmas which deserves careful consideration. Present applications of RBQ and NUBEAM to ITER steady state case have shown a weak loss of fast ions to the wall at the level of a few percent.

Acknowledgments. Discussions with Prof. G.-Y. Fu concerning long term evolution of AEs are appreciated. This work was supported by the US Department of Energy under contract DE-AC02-09CH11466.

Appendix A: AE continuum damping

Continuum damping calculations are important for relatively low toroidal mode number AEs [22]. It has been shown that perturbative calculations of this damping may have convergence issues [42]. A detailed study of FLR and AE nonperturbative effects on the continuum damping has been published elsewhere [43].

As it was shown in Ref. [22] a rough formula for the continuum damping rate can be derived for the magnetic shear value $|s| > 0.3$ and when $1 < m\varepsilon < 20$. The following expression is valid within a factor of 2:

$$\frac{\gamma_c}{\omega} = -\frac{0.8s^2}{\sqrt{m^3\varepsilon}}. \tag{A1}$$

As it follows from our calculations the most unstable AEs which can contribute to EP relaxation exist near q_{min} and toward the plasma center. Maximum magnetic shear value in that region is $|s| \leq 1$ (see Fig.1) and thus $-\gamma_c/\omega \lesssim 2\times 10^{-2}$ over the range of expected toroidal mode numbers. Recent analysis of JET DT experiments confirms this assessment using the kinetic CASTOR-K simulations [44].

[1] N. N. Gorelenkov and V. N. Duarte, Phys. Lett. A **386**, 126944 (2021).

[2] D. C. Pace, M. E. Austin, E. M. Bass, R. V. Budny, W. W. Heidbrink, J. C. Hillesheim, C. T. Holcomb, M. Gorelenkova, B. A. Grierson, D. C. McCune, G. R. McKee, C. M. Muscatello, J. M. Park, C. C. Petty, T. L. Rhodes, G. M. Staebler, T. Suzuki, M. A. Van Zeeland, R. E. Waltz, G. Wang, A. E. White, Z. Yan, X. Yuan, and Y. B. Zhu, Phys. Plasmas **20**, 056108 (2013).

[3] J. Jacquinot, S. Putvinski, and e. G. Bosia, Nucl. Fusion **39**, 2471 (1999).

[4] N. N. Gorelenkov, W. W. Heidbrink, G. J. Kramer, J. B. Lestz, M. Podestà, M. A. Van Zeeland, and R. B. White, Nucl. Fusion **56**, 112015 (2016).

[5] R. E. Waltz, E. M. Bass, W. W. Heidbrink, and M. Van Zeeland, Nucl. Fusion **55**, 123012 (2015).

[6] N. N. Gorelenkov, V. N. Duarte, C. S. Collins, M. Podestà, and R. B. White, Phys. Plasmas **26**, 072507 (2019).

[7] N. N. Gorelenkov, C. Z. Cheng, and G. Y. Fu, Phys. Plasmas **6**, 2802 (1999).

[8] J. Lang and G.-Y. Fu, Phys. Plasmas **18**, 055902 (2011).

[9] N. N. Gorelenkov, H. L. Berk, and R. V. Budny, Nucl. Fusion **45**, 226 (2005).

[10] S. D. Pinches, I. T. Chapman, P. W. Lauber, H. Oliver, S. E. Sharapov, K. Shinohara, and K. Tani, Phys. Plasmas **22**, 021807 (2015).

[11] S. Taimourzadeh, E. M. Bass, Y. Chen, C. Collins, N. N. Gorelenkov, A. Könies, Z. X. Lu, D. A. Spong, Y. Todo, M. E. Austin, J. Bao, M. Borchardt, A. Bottino, W. W. Heidbrink, Z. Lin, R. Kleiber, A. Mishchenko, L. Shi, J. Varela, R. E. Waltz, G. Yu, W. L. Zhang, and Y. Zhu, Nucl. Fusion **59**, 066006 (2019).

[12] N. N. Gorelenkov and S. V. Putvinskii, Fiz. Plasmy [Sov.J.Plasma Phys **15**, 145 (1989)] **18**, 145 (1989).

[13] N. N. Gorelenkov, S. D. Pinches, and K. Toi, Nucl. Fusion **54**, 125001 (2014).

[14] C. Z. Cheng and M. S. Chance, Phys. Fluids **29**, 3695 (1986).

[15] A. R. Polevoi, A. A. Ivanov, S. Y. Medvedev, G. T. A. Huijsmans, S. H. Kim, A. Loarte, E. Fable, and A. Y. Kuyanov, Nucl. Fusion **60**, 096024 (2020).

[16] F. Imbeaux, S. D. Pinches, J. B. L. amd Y. Buravand, T. Casper, B. Duval, B. Guillerminet, M. Hosokawa, W. Houlberg, P. Huynh, S. H. Kim, G. Manduchi, M. Owsiak, B. Palak, M. Plociennik, G. Rouault, O. Sauter, and P. Strand, Nucl. Fusion **55**, 123006 (2015).

[17] Z. Lin, E. Bass, G. Brochard, Y. Ghai, N. N. Gorelenkov, M. Idouakass, C. Liu, P. Liu, M. Podestà, D. Spong, X. Wei, W. Heidbrink, G. McKee, R. Waltz, J. Bao, B. Cornille, V. N. Duarte, R. Falgout, M. V. Gorelenkova, T. Hayward-Schneider, S. H. Kim, W. Joubert, S. Klasky, I. Lyngaas, K. Mehta, J. Nicolau, S. Pinches, A. Polevoi, M. Schneider, G. Sitaraman, W. Tang, P. Wang, and S. Williams, in *Proceedings of 29th IAEA Fusion Energy Conference, London, United Kingdom*, IAEA-CN-316-2295/TH-W/2-2 (2023) pp. 1–9.

[18] M. Fitzgerald, S. E. Sharapov, P. Rodrigues, and D. Borba, Nucl. Fusion **56**, 112010 (2016).

[19] M. Schneller, P. Lauber, M. Brüdgam, S. D. Pinches, and S. Günter, Plasma Phys. Control Fusion **58**, 014019 (2016).

[20] R. B. White, R. J. Goldston, M. H. Redi, and R. V. Budny, Phys. Plasmas **3**, 3043 (1996).

[21] Y. Zou, V. S. Chan, M. A. V. Zeeland, W. W. Heidbrink, Y. Todo, W. Chen, Y. Wang, and J. Chen, Phys. Plasmas **29**, 032304 (2022).

[22] M. N. Rosenbluth, H. L. Berk, J. W. Van Dam, and D. M. Lindberg, Phys. Fluids B **4**, 2189 (1992).

[23] A. Pankin, D. McCune, R. Andre, and et al., Comp. Phys. Communications **159**, 157 (2004).

[24] R. B. White, *The Theory of Toroidally Confined Plasmas*, 3rd ed. (Imperial College Press, London, UK, 2013).

[25] N. N. Gorelenkov, V. N. Duarte, M. Podesta, and H. L. Berk, Nucl. Fusion **58**, 082016 (2018).

[26] A. N. Kaufman, J. Plasma Phys. **8**, 1 (1972).

[27] V. N. Duarte, *Quasilinear and nonlinear dynamics of energetic-ion-driven Alfvén eigenmodes, http://www.teses.usp.br/teses/disponiveis/43/43134/tde-01082017-195849/*, Ph.D. thesis, University of São Paulo, Brazil (2017).

[28] V. N. Duarte, J. B. Lestz, N. N. Gorelenkov, and R. B. White, Phys. Rev. Lett. **130**, 105101 (2023).
[29] J. Fitzpatrick, *A Numerical Model of Wave-Induced Fast Particle Transport in a Fusion Plasma*, Ph.D. thesis, University of California, Berkeley, Berkeley, CA (1997).
[30] H. L. Berk, B. N. Breizman, J. Fitzpatrick, and H. V. Wong, Nucl. Fusion **35**, 1661 (1995).
[31] V. N. Duarte, N. N. Gorelenkov, R. B. White, and H. L. Berk, Phys. Plasmas **26**, 120701 (2019).
[32] K. Ghantous, H. L. Berk, and N. N. Gorelenkov, Phys. Plasmas **21**, 032119 (2014).
[33] H. L. Berk, B. N. Breizman, and H. Ye, Phys. Rev. Lett. **68**, 3563 (1992).
[34] M. V. Gorelenkova, A. Pankin, N. N. Gorelenkov, M. L. Podesta, V. N. Duarte, J. A. Breslau, L. Glant, M. Goliyad, G. Perumpilly, J. Sachdev, and F. M. Poli, Bull. Amer. Phys. Society (abstract UP11.00010) **64**, https://meetings.aps.org/Meeting/DPP22/Session/UP11.10 (2022).
[35] V. N. Duarte, H. L. Berk, N. N. Gorelenkov, W. W. Heidbrink, G. J. Kramer, R. Nazikian, D. C. Pace, M. Podestà, and M. A. Van Zeeland, Phys. Plasmas **24**, 122508 (2017).
[36] M. Podestà, M. V. Gorelenkova, and R. B. White, Plasma Phys. Control. Fusion **56**, 055003 (2014).
[37] C. Angioni, A. G. Peeters, G. V. Pereverzev, A. Botino, J. Candy, R. Dux, E. Fable, E. Hein, and R. E. Waltz, Nucl. Fusion **49**, 055013 (2009).
[38] W. W. Heidbrink, C. S. Collins, M. Podestà, G. J. Kramer, D. C. Pace, C. C. Petty, L. Stagner, M. A. Van Zeeland, R. B. White, and Y. B. Zhu, Phys. Plasmas **24**, 056109 (2017).
[39] S. Pinches, V. Kiptily, S. Sharapov, D. Darrow, L.-G. Eriksson, H.-U. Fahrbach, M. Garcia, M. Reich, E. Strumberger, A. Werner, the ASDEX Upgrade Team, and J.-E. Contributors, Nuclear Fusion **46**, S904 (2006).
[40] F. Procelli, R. Stankiewicz, W. Kerner, and H. L. Berk, Phys. Plasmas **1**, 470 (1994).
[41] Y. Chen, G. Y. Fu, C. Collins, S. Taimourzadeh, and R. B. White, Phys. Plasmas **25**, 032304 (2018).
[42] G. W. Bowden, A. Koenies, M. J. Hol, N. N. Gorelenkov, and G. R. Dennis, Phys. Plasmas **21**, 052508 (2014).
[43] N. N. Gorelenkov, L. Yu, Y. Wang, and G. Fu, J. Plasma Phys **89** (submitted 2024).
[44] M. Fitzgerald, R. Dumont, D. Keeling, J. Mailloux, S. Sharapov, M. Dreval, A. Figueiredo, R. Coelho, J. Ferreira, P. Rodrigues, F. Nabais, D. Borba, Å. Å tancar, G. Szepesi, R. A. Tinguely, P. G. Puglia, H. J. C. Oliver, V. Kiptily, M. Baruzzo, M. Lennholm, P. Siren, J. Garcia, C. F. Maggi, and JET Contributors, Nucl. Fusion **63**, 112006 (2023).